Optimization of Gaussian basis sets for density-functional calculations

Dirk Porezag and Mark R. Pederson
Center for Computational Materials Science, Naval Research Laboratory, Washington, D.C. 20375
(Received 19 April 1999)

We introduce a scheme for the optimization of Gaussian basis sets for use in density-functional calculations. It is applicable to both all-electron and pseudopotential methodologies. In contrast to earlier approaches, the number of primitive Gaussians (exponents) used to define the basis functions is not fixed but adjusted, based on a total-energy criterion. Furthermore, all basis functions share the same set of exponents. The numerical results for the scaling of the shortest-range Gaussian exponent as a function of the nuclear charge are explained by analytical derivations. We have generated all-electron basis sets for H, B through F, Al, Si, Mn, and Cu. Our results show that they efficiently and accurately reproduce structural properties and binding energies for a variety of clusters and molecules for both local and gradient-corrected density functionals.
[S1050-2947(99)07110-3]

PACS number(s): 31.15.Ew

I. INTRODUCTION

The majority of all electronic-structure methods that are currently used to investigate extended systems expands the electronic wave functions in terms of basis functions. Two classes of functions are commonly applied: plane waves (PWs) and localized atomiclike orbitals (AOs). PW basis sets are usually applied in combination with pseudopotentials for supercell calculations with periodic boundary conditions [1]. They are computationally easy to handle and the convergence of the calculated properties with respect to basis-set size can be controlled easily. However, they suffer from the drawback that many basis functions are needed to accurately describe localized states. As a result, calculations on systems of first-row or transition-metal atoms can be quite expensive. Atomiclike orbitals provide an excellent tool for bypassing these problems since they are intrinsically localized. Furthermore, it should be noted that there is currently much progress in developing self-consistent full-potential methods, which scale linearly with system size [2–4]. Such methods are much more easily implemented within a localized basis since well-separated, localized orbitals do not overlap.

Several types of AO functions have been proposed. Commonly used are augmented plane waves [5] that are actually a mix of plane waves and AOs, linearized muffin-tin orbitals [6], Slater-type orbitals (STOs) introduced by Slater [7], and Gaussian-type orbitals (GTOs) which were first used by Boys [8]. STOs describe the properties of the atomic wavefunctions more accurately than GTOs but the mathematics associated with them is much more involved. The advantages of STOs and GTOs may be combined by building linear combinations of GTOs, which resemble the shape of STOs. These basis functions are called contracted GTOs (CGTOs). The usefulness of GTOs in calculations on finite systems such as molecules and clusters was first demonstrated by Huzinaga [9] and their importance has been growing ever since [10–18]. Most of the early work aimed at constructing CGTOs was based on least-squares fitting [9,19–21]. Later, Tatewaki and Huzinaga [22] combined least-squares fits and an atomic optimization scheme to obtain more reliable basis sets. This method was also used later by Andzelm and coworkers [14,23] to create a set of density-functional optimized CGTOs. More sophisticated Hartree-Fock-based optimization schemes, which avoid least-squares fits, have also been developed [24,25].

Experience has shown that it is a good idea to base the construction of CGTOs on calculations for free atoms. The general philosophy is to find the best set of CGTOs for the free atom and then provide additional functions to allow the atom to respond to changes in its environment. The majority of the previously reported methods for constructing CGTOs have the disadvantage that they fix the number of GTOs used to define a single CGTO. This may lead to deficiencies in the description of the core or valence orbitals of a given atom. As a result, functions corresponding to other atoms may lower its energy further when it is placed into a molecule, thus resulting in an overestimation of the binding energy. This effect is called basis-set superposition error (BSSE). Furthermore, different atomic orbitals are usually optimized independently, which leads to a different set of Gaussian exponents for each orbital. In practical applications, one expensive part of the calculation is the evaluation of the exponential function or its integrals (for instance, for the determination of the wave function or Coulomb energy), while the degree of the contraction is less important. For this reason, a basis set, which uses the same set of exponents for all CGTO orbitals, is more desirable since it is more efficient. We have developed a method to construct such basis sets. It is described in Sec. II. In Sec. III, we show that these basis sets are able to yield converged results for equilibrium properties of a variety of systems ranging from simple first-row atom molecules to magnetic transition metal-oxide clusters. The basis-set exponents and coefficients for all elements discussed here are given in Ref. [26]. We hope that they will facilitate future work with Gaussian orbital basis sets and further increase the number of research groups using this approach.

II. METHOD

The basis-set optimization scheme introduced here is applied within the density-functional formalism (DFT) [27,28]

but it could be used in principle within Hartree-Fock or other methods. If density-functional theory is applied within the usual Kohn-Sham scheme, the total energy can be written as

$$E=\sum_{\sigma,i}^{occ} n_{i\sigma}\int d\boldsymbol{r}\,\Phi_{i\sigma}^{*}(\boldsymbol{r})\left[-\frac{\boldsymbol{\nabla}^2}{2}+V_{ext}(\boldsymbol{r})+V_H[\rho(\boldsymbol{r})]\right]\Phi_{i\sigma}(\boldsymbol{r}) + E_{xc}[\rho_{\uparrow}(\boldsymbol{r}),\rho_{\downarrow}(\boldsymbol{r})], \tag{1}$$

where σ denotes the spin index, $n_{i\sigma}$ are the occupation numbers, $\Phi_{i\sigma}$ are the Kohn-Sham orbitals, V_H is the Coulomb potential due to the electron density ρ, and E_{xc} is the exchange-correlation energy depending on the spin densities $\rho_{\uparrow}$ and $\rho_{\downarrow}$ given by

$$\rho_{\sigma}(\boldsymbol{r})=\sum_{i}^{occ}\Phi_{i\sigma}^{*}(\boldsymbol{r})\Phi_{i\sigma}(\boldsymbol{r}),\quad \rho(\boldsymbol{r})=\rho_{\uparrow}(\boldsymbol{r})+\rho_{\downarrow}(\boldsymbol{r}). \tag{2}$$

The Kohn-Sham orbitals are determined by minimizing total-energy expression (1), which leads to the Kohn-Sham equations:

$$\left[-\frac{\boldsymbol{\nabla}^2}{2}+V_{ext}(\boldsymbol{r})+V_H[\rho(\boldsymbol{r})]+V_{xc}[\rho_{\uparrow}(\boldsymbol{r}),\rho_{\downarrow}(\boldsymbol{r})]\right]\Phi_{i\sigma}(\boldsymbol{r}) =\varepsilon_{i\sigma}\Phi_{i\sigma}(\boldsymbol{r}), \tag{3}$$

where V_{xc} is the functional derivative of E_{xc}.

A. Determination of the Gaussian exponents

The Gaussian exponents are optimized by minimizing the total energy of the spherical free atom in its electronic ground state. For this system, radial and angular degrees of freedom may be separated. The radial wave functions still need to be determined while the angular part is given by spherical harmonics. We expand the ith atomic Kohn-Sham orbital corresponding to angular momentum (l,m) into GTOs $\varphi_{lm\alpha}$ given by

$$\Phi_{ilm\sigma}=\sum_{\alpha}c_{li\sigma\alpha}\varphi_{lm\alpha}(\boldsymbol{r}),\quad \varphi_{lm\alpha}(\boldsymbol{r})=r^{l}e^{-\alpha r^2}Y_{lm}\left(\frac{\boldsymbol{r}}{r}\right). \tag{4}$$

The total energy of the spherical atom may then be expressed as

$$E=\sum_{\sigma}\sum_{l}\sum_{i}^{occ}n_{li\sigma}\sum_{\alpha'}\sum_{\alpha}c_{li\sigma\alpha'}c_{li\sigma\alpha}\int_0^{\infty}dr\,r^{l+2}e^{-\alpha' r^2} \times\left[-\frac{\nabla_r^2}{2}+\frac{l(l+1)}{2r^2}-\frac{Z}{r}+\frac{1}{2}V_H[\rho(r)] +\varepsilon_{xc}(\rho_{\uparrow}(r),\rho_{\downarrow}(r))\right]r^{l}e^{-\alpha r^2}, \tag{5}$$

where the occupation numbers $n_{li\sigma}$ may range from 0 to $2l+1$ due to angular momentum degeneracies. ∇_r^2 is the radial part of the Laplacian operator given by $\nabla_r^2=d^2/dr^2+(2/r)d/dr$. The Coulomb potential of the nucleus $-Z/r$ may be replaced by a (possibly l-dependent) pseudopotential if basis bets are to be optimized for this technique.

Total-energy expression (5) only depends on the exponents α and coefficients $c_{li\sigma\alpha}$. For a given number of exponents, one needs to search for the set of exponents and coefficients that leads to the lowest total energy. For a given set $\{\alpha\}$ the best $c_{li\sigma\alpha}$ can be determined by performing a standard self-consistent solution of the atomic problem within the DFT framework. After a successful atomic calculation with a fixed set of exponents we calculate the derivatives G_{α} of the total energy with respect to α given by

$$G_{\alpha}=-2\sum_{\sigma}\sum_{l}\sum_{i}^{occ}n_{li\sigma}c_{li\sigma\alpha}\sum_{\beta}c_{\beta li\sigma}\int_0^{\infty}dr\,r^{l+4}e^{-\alpha r^2} \times\left[-\frac{\nabla_r^2}{2}+\frac{l(l+1)}{2r^2}-\frac{Z}{r}+V_H[\rho(r)] +V_{xc}(\rho_{\uparrow}(r),\rho_{\downarrow}(r))-\varepsilon_{li\sigma}\right]r^{l}e^{-\beta r^2}. \tag{6}$$

The knowledge of G_{α} enables one to use efficient conjugate-gradient routines to minimize the total energy with respect to α. Derivatives of the DFT total energy with respect to Gaussian exponents have been previously used in molecular DFT simulations [29]. Note that Eq. (6) is the full (as opposed to partial) derivative of the total energy with respect to α. This is the case since for a fully self-consistent solution of the atomic Kohn-Sham equations, the derivative of the total energy with respect to $c_{li\sigma\alpha}$ is zero and hence the Hellmann-Feynman theorem can be applied to calculate the G_{α}.

Since the necessary theory is now developed, our strategy to optimize the Gaussian exponents based on an atomic calculation may be pointed out. (a) Perform a basis set free (all numerical) atomic calculation in order to find the correct ground-state energy. (b) Define the total number of exponents. (c) Define the initial set of exponents $\{\alpha\}$. By default, this is a geometric progression (even-tempered Gaussians) ranging from $\alpha=0.05$ to $\alpha=100\ Z^3$. Of course, the final result of the optimization should not depend on the initial guess and we find that this is indeed the case. (d) Find the atomic ground-state energy in a self-consistent DFT calculation. (e) Calculate the derivatives G_{α} of the total energy with respect to each exponent α via Eq. (6). (f) Compute the natural logarithm $(\ln\alpha)$ and $G_{\ln\alpha}=(\partial E/\partial\ln\alpha)=\alpha G_{\alpha}$ for each exponent α. If the $G_{\ln\alpha}$ are larger than the predefined convergence margin, use a conjugate gradient routine to update $\{\ln\alpha\}$ and go back to step (d). Optimizing $\{\ln\alpha\}$ instead of $\{\alpha\}$ is numerically more stable and therefore advantageous. (g) Compare the total energy with the result of step (a). If the difference is larger than a predefined error margin, increase the number of exponents and go back to step (c).

One fact worth pointing out is that different α may ''attract'' each other in the course of an optimization. This can lead to instabilities in the relaxation process due to linear dependences in the basis set. To avoid this problem, an auxiliary term is added to the total energy:

$$E_{aux}=\sum_{\alpha}\sum_{\alpha'\neq\alpha}\begin{cases}\dfrac{a}{x}(1-x)^3 & (x\leqslant 1),\\ 0 & (x\geqslant 1),\end{cases} \tag{7}$$

where

$$x=\left(\frac{\ln(\alpha)-\ln(\alpha')}{\ln(b)}\right)^2.$$

We have chosen to fix $a=0.1$ eV, $b=1.5$. All basis sets published here have been derived with this setting without encountering any problems in the optimization. Furthermore, for the cases presented here E_{aux} always vanishes for the final set of exponents, i.e., it is only needed to stabilize the minimization procedure.

One fact worth discussing is the scaling behavior of the largest exponent $A\equiv\alpha_{max}$ as a function of the nuclear charge Z. Numerically, we find that A is approximately proportional to $Z^{3.3}$. It can be expected that this scaling is closely connected to the properties of the $1s$ core state, which may be well approximated by the corresponding $1s$ orbital of a one-electron hydrogenlike atom with nuclear charge Z. This system is described by the Hamiltonian:

$$\hat{H}=-\frac{\boldsymbol{\nabla}^2}{2}-\frac{Z}{r}, \tag{8}$$

which is invariant with respect to a renormalization $\boldsymbol{r}\rightarrow\boldsymbol{r}/Z$ and $E\rightarrow EZ^2$ of spatial coordinate and energy. Based on this knowledge one can show that a (possibly incomplete) Gaussian basis set, which predicts an energy E_H for the hydrogen atom ($Z=1$), will give an energy E_HZ^2 for arbitrary Z if the Gaussian exponents are scaled as $\alpha=\alpha_HZ^2$ ($\sqrt{\alpha}$ has the dimension of an inverse length). This is also true for the largest exponent A and, therefore,

$$\varepsilon=E-E^0=(E_H-E_H^0)Z^2=\varepsilon_HZ^2,\quad A=A_HZ^2, \tag{9}$$

where ε is the difference between actually calculated and ground-state energy (E and E^0, respectively) due to basis-set incompleteness. Focusing our attention on the hydrogen atom ($Z=1$), we can write a Gaussian basis-set expansion of the radial wave function $\Phi(r)$ in the most general form as

$$\Phi(r)=\int_0^{A_H}d\alpha\, c(A_H,\alpha)\exp(-\alpha r^2), \tag{10}$$

where A_H is the largest exponent allowed in the expansion. For $A_H=\infty$ (complete basis), $c(\infty,\alpha)$ is known [9]:

$$c(\infty,\alpha)\sim\alpha^{-3/2}\exp\left(-\frac{1}{4\alpha}\right). \tag{11}$$

For arbitrary A_H, the $c(A_H,\alpha)$ which leads to the lowest energy, can be obtained by requiring that the variation

$$\frac{\delta}{\delta c(A_H,\alpha)}E_H=\frac{\delta}{\delta c(A_H,\alpha)}\langle\Phi|\hat{H}|\Phi\rangle=0,\quad\langle\Phi|\Phi\rangle=1. \tag{12}$$

After substituting $B_H=1/\sqrt{A_H}$ it is possible to expand the energy E_H at $B_H=0$. Using straightforward differentiation and Eqs. (10)–(12) one concludes that the first- and second-order derivatives vanish and, therefore,

$$\varepsilon_H=E_H-E_H^0\sim B_H^3\sim A_H^{-3/2}. \tag{13}$$

We have also veryfied Eq. (13) numerically by determining the total energy of the hydrogen atom with Gaussian basis sets. Finally, combining Eqs. (9) and (13) results in

$$\varepsilon\sim A^{-3/2}Z^5\quad\text{or}\quad A\sim\varepsilon^{-2/3}Z^{10/3}. \tag{14}$$

The above equation predicts an analytically derived scaling of A proportional to $Z^{10/3}$, which agrees well with the $Z^{3.3}$ scaling found numerically.

B. Determination of the contraction coefficients

After the optimum Gaussian exponents α have been found, the first set of CGTOs is defined by building a minimal basis set (one CGTO each for $1s$, $2s$, $2p$, $3s$, $3p$, $3d$, etc.) for the free atom. We are already furnished with a GTO expansion of these orbitals (the $c_{\alpha li\sigma}$ obtained in the α optimization contain exactly the information we need). The only complication is that instead of a single expansion for each state, there are two (spin up and down) similar but different sets of $c_{li\sigma\alpha}$. Therefore, the spin-averaged orbitals are constructed from

$$\Phi_{lmi}=\sum_{\alpha}c_{li\alpha}\varphi_{lm\alpha},\quad c_{li\alpha}=\frac{n_{li\uparrow}c_{li\uparrow\alpha}+n_{li\downarrow}c_{li\downarrow\alpha}}{n_{li\uparrow}+n_{li\downarrow}}, \tag{15}$$

which will give the majority spin orbital for a fully spin-polarized state and the correct spin-averaged orbitals for a spinless state.

Although the $c_{li\alpha}$ resulting from Eq. (15) would provide a very good minimal basis set for the atom, they do have a major disadvantage. Since they were determined based on an atomic all-electron calculation, the valence states show the usual wiggles close to the nucleus. In order to accurately represent these wiggles one needs GTOs with fairly large Gaussian exponents (similar to the ones needed for the core states). However, it would be preferable to have a set of basis functions that are either short-range (core) or long-range (valence) without any substantial wiggles. Fortunately, it is possible to create a new set Φ'_{lmi} of CGTOs with the desired properties as a linear combination of the old Φ_{lmi} defined by Eq. (15) without losing accuracy since the total energy will not change as long as the Φ'_{lmi} span the same space as the Φ_{lmi}.

The basis-set transformation is done independently for each angular momentum. Assuming that the old states Φ_{lmi} are ordered so that their Kohn-Sham eigenvalues (and spatial range) increase with increasing state index, the Φ'_{lmi} are written as

$$\Phi'_{lmi}=\sum_{j}^{i}d_{lij}\Phi_{lmj}\rightarrow c'_{li\alpha}=\sum_{j}^{i}d_{lij}c_{li\alpha} \tag{16}$$

and the d_{lij} are determined so the expression

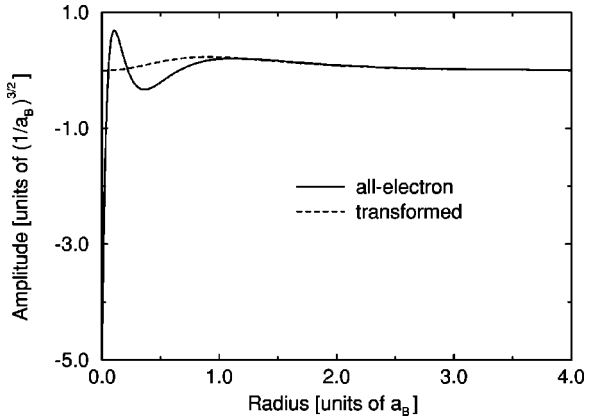

FIG. 1. All-electron Kr 4*s* orbital and the smooth function resulting from the orbital transformation described in Sec. II.

$$\sum_j \sum_{j'} d_{lij} d_{lij'} \sum_\alpha \sum_{\alpha'} c_{li\alpha} c_{li\alpha'} \langle \varphi_{lm\alpha} | \varphi_{lm\alpha'} \rangle (\alpha\alpha')^{3/2} \tag{17}$$

is minimized under the condition that the Φ'_{lmi} remain normalized. Although this procedure is certainly not unique, it effectively reduces the contribution of large Gaussian exponents to Φ'_{lmi}. Consequently, the contribution of many $c'_{li\alpha}$ to Φ'_{lmi} is now negligible. As a result, the final basis functions contain fewer terms in the CGTO expansion, which further increases their efficiency for large-scale calculations. Figure 1 shows how the Krypton 4*s* orbital can be transformed into a very smooth orbital by means of the procedure described above.

While the set $\{\Phi'_{lmi}\}$ of CGTOs is well suited for the free atom in its ground state, it is an overconstrained basis set for clusters, molecules, and solids, because in these systems the valence electrons usually assume a spatial distribution, which is different from the free atom. The basis that has been constructed so far does not give the valence electrons the freedom to ''breathe'' since they are ''frozen'' in a single CGTO. This deficiency may be overcome by creating additional functions allowing the atoms to adapt to changes in their environment. These functions may be of higher angular momentum than the ones occupied in the atom (polarization functions) or just provide more radial flexibility (breathing functions).

In order to keep the extended basis as efficient as possible, the Gaussian exponents resulting from the optimization scheme described above may also be used to form the additional CGTOs. This is not a serious restriction since adjacent α values are not too different and intermediate values may be approximated well by linear combinations. The additional CGTOs are optimized by minimizing the total energy of the homonuclear diatomics at their equilibrium separation. This way, the optimization of all basis functions is based on the same simple criterion. However, in a few cases the homonuclear diatomics are either unbound or very weakly bound. In these cases, heteronuclear diatomics may be more suitable (e.g., Mn-O has been used here to optimize the additional functions for Mn) or the internuclear separation needs to be chosen manually at a reasonable value.

For the smallest of the basis sets presented here [denoted density-functional optimized (DFO-1) in the next section], we have chosen to define one additional CGTO per angular momentum comprised of two GTOs. This corresponds to a level usually referred to as double-zeta valence with polarization function similar to the 6-31G* basis used by many commercial program packages [13]. For increased accuracy, more single GTOs may be added to the basis. In this manner, one can gradually obtain basis sets with more and more functions and higher accuracy.

III. RESULTS AND DISCUSSION

In this paper, we report all-electron basis sets and results for the elements H,B through F, Al, Si, Mn, and Cu. We also provide a function set for Si applicable in calculations using Bachelet-Haman-Schlüter pseudopotentials [30,31]. Of course, the same procedure may be applied to other elements as well. All basis sets were optimized within the local-density approximation (LDA) but results are also presented for the Perdew-Burke-Ernzerhof (PBE) generalized gradient approximation (GGA) [34,35]. The code for the basis set construction is available from the authors via the World Wide Web (please contact porezag@physics.georgetown.edu for details). Results for clusters and molecules have been obtained using a Gaussian orbital-based cluster code (NRLMOL) developed by Pederson and Jackson [15,16]. Within this scheme, all necessary integrals are determined numerically using a variational mesh, which allows for arbitrary precision. Furthermore, densities and potentials are calculated directly from the wave functions without using any additional expansions or approximations.

Three different basis sets are used in this paper for each atomic species. They are termed DFO-X. DFO-1 was constructed with an error margin of 0.1 eV in the optimization of the exponents, one additional breathing function per angular momentum, and one polarization function. DFO-2 was created with an error margin of 0.01 eV, two additional breathing functions per angular momentum, and two polarization functions. DFO-R is only used to assess the quality of DFO-1 and DFO-2 in terms of convergence with basis-set size. It contains the same Gaussian exponents as DFO-2 plus one additional Gaussian exponent, which is one third of the longest-range DFO-2 exponent. However, in contrast to DFO-2, which uses these GTOs to define contracted functions, DFO-R employs all exponents smaller than 10.0 a.u. as single GTOs. It is therefore very flexible. Hyperpolarization functions (of angular momentum $l+2$ where l is the highest angular momentum occupied in the free atom) have not been included in either of the basis sets. While it is known that orbitals of this type may be important to obtain converged results for properties that depend on the response of the electrons to external perturbations such as electric fields [32,33], they usually have a very small impact on binding energies and structural properties, which are the main issue in this paper. In certain cases, hyperpolarization functions may also be replaced by off-center CGTOs of lower angular momentum.

The results are compared with two basis set types known from the literature and commonly used today: the sets published by Andzelm, Godbout (AG), and co-workers [14,23]

TABLE I. RMS errors (in eV) with respect to all-numerical calculations for LDA total energies and eigenvalues of the occupied valence states calculated within the DFO and other basis sets. AG basis sets are from Refs. [14,23] and 6-31G* sets are from Ref. [13].

Atoms	Quantity	DFO-R	DFO-2	DFO-1	AG	6-31G*
H	ΔE_{tot}	0.001	0.001	0.021	0.062	0.254
	$\Delta \varepsilon_v$	0.000	0.002	0.028	0.210	0.504
B–F	ΔE_{tot}	0.007	0.009	0.089	0.154	0.986
	$\Delta \varepsilon_v$	0.001	0.003	0.040	0.061	0.668
Al	ΔE_{tot}	0.009	0.011	0.093		0.873
	$\Delta \varepsilon_v$	0.001	0.003	0.049		0.049
Si	ΔE_{tot}	0.010	0.012	0.124		0.980
	$\Delta \varepsilon_v$	0.002	0.003	0.043		0.080
Mn	ΔE_{tot}	0.008	0.013	0.083	30.503	
	$\Delta \varepsilon_v$	0.000	0.003	0.018	0.055	
Cu	ΔE_{tot}	0.010	0.011	0.097	44.380	
	$\Delta \varepsilon_v$	0.001	0.006	0.060	0.133	

(defined for H,B through F, and Sc through Zn) that were optimized within DFT, and the 6-31G* set (defined for H through Ar), which is based on the work of Pople and coworkers [36] and probably one of most widely used Gaussian basis sets in general. It should be noted that in contrast to all other basis sets discussed here 6-31G* has been optimized based on Hartree-Fock calculations and proven to be efficient and accurate for these types of calculations. DFT and Hartree-Fock frequently show a different spatial behavior of the charge density and we would like to stress that the DFT results published here cannot be used to assess the quality of the basis sets for Hartree-Fock or other methods.

Since the main purpose of this paper is to demonstrate the convergence of the calculation with basis-set size, all calculated quantities will be compared to the corresponding DFO-R results. In other words, we want to show the magnitude of the basis set expansion errors for different quantities. Deviations between theory and experiment that are caused by the theory (DFT) itself are beyond the scope of this publication. There are a number of papers available that address this issue [34,37,38].

A. Atoms

The total energy of the free atoms was the main figure of merit used in the basis-set optimization. Therefore, one should expect good results for these systems. Table I shows the root-mean-square (RMS) errors for total energies and Kohn-Sham eigenvalues of the occupied valence orbitals with respect to basis-set free numerical calculations. The results are determined within the LDA using the (spin-polarized) electronic ground-state configurations. As expected, the accuracy decreases in the order DFO-R, DFO-2, and DFO-1. However, all DFO sets remain approximately within the error margins set in the optimization (0.1 eV for DFO-1 and 0.01 eV for DFO-2, respectively). For hydrogen, the DFO sets perform significantly better than AG and much better than 6-31G*. The main reason for the errors associated with the latter sets is that they do not provide a sufficiently long-range *s*-type function. For the first-row elements B through F, DFO-1 shows a slightly better performance than AG and both of these sets are much better than 6-31G*. Large differences between DFO-1 and AG can be observed for the total energies of the heavy Mn and Cu atoms. This is mainly due to the fact that the AG CGTOs are comprised of only 4 GTOs for these atoms in order to keep the numerical efforts tractable. However, it is worth noting that the AG set for Mn still contains 26 different exponents while DFO-1 and DFO-2 contain only 17 and 20, respectively. One of the advantages of the present basis-set optimization scheme is that the number of Gaussian exponents does not grow linearly with the number of occupied states in the atom, but it grows logarithmically with its nuclear charge (of course this behavior will change if pseudopotentials are employed instead of performing an all-electron calculation).

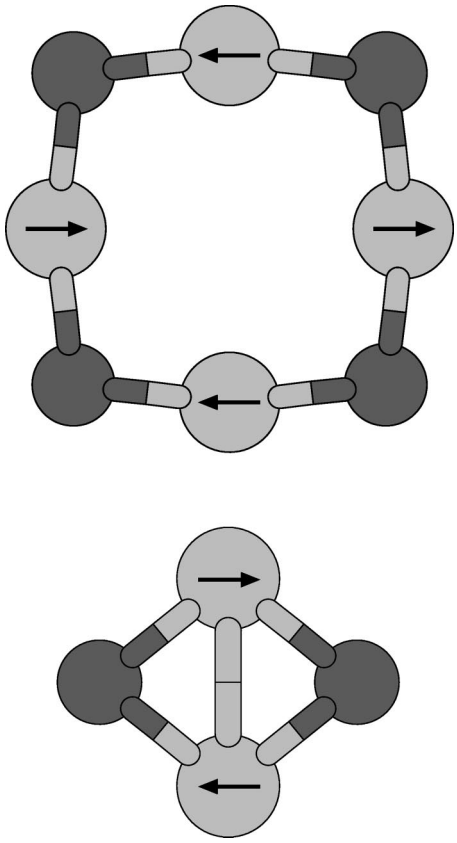

FIG. 2. GGA-PBE ground-state structures of the Mn_2O_2 and Mn_4O_4 clusters. The arrows indicate the spin of the manganese $3d$ electrons and indicate an antiferromagnetic ordering.

B. Bond lengths and angles

We have tried to select a variety of systems with different types of bonding to demonstrate the basis-set performance. The set includes the simple diatomic H_2, CH_4 (methane), C_2H_6 (ethane), C_2H_4 (ethene), and C_2H_2 (acetylene) as examples for hydrocarbons with single, double, and triple bonds. C_{60} as the most important fullerene cluster, H_2O (water), HCN (hydrogen cyanide), HCF_3 (fluoroform), and trans-HCOOH (formic acid), as examples for systems with a fairly large interatomic charge transfer, have also been investigated. Si_2H_6 (disilane), which has a simple Si-Si single

TABLE II. Dipole moments (D) as calculated with different basis sets. Experimental data for H_2O and HCN are from Ref. [37], for HCF_3 and HCOOH from Ref. [42]. AG basis sets are from Refs. [14,23] and 6-31G* sets are from Ref. [13].

		LDA					GGA-PBE				
	Exp.	DFO-R	DFO-2	DFO-1	AG	6-31G*	DFO-R	DFO-2	DFO-1	AG	6-31G*
H_2O	1.85	1.86	1.89	2.12	2.16	2.07	1.81	1.84	2.06	2.08	1.99
HCN	2.98	3.03	3.03	3.02	3.00	2.91	2.96	2.96	2.98	2.93	2.84
HCF_3	1.59	1.53	1.53	1.58	1.68	1.31	1.54	1.53	1.59	1.68	1.32
HCOOH	1.51	1.54	1.55	1.51	1.59	1.52	1.48	1.49	1.45	1.53	1.47

bond, is also part of the set. Additionally, we have included the planar rhombus-shaped Si_4 cluster (for previous theoretical investigation see, e.g., Refs. [39–41] and the manganese oxide clusters Mn_2O_2 and Mn_4O_4). To the best of our knowledge, there have been no previous theoretical investigations of these transition-metal oxide clusters. Their ground state is found to be planar with an antiferromagnetic ordering of the manganese $3d$ electrons (see Fig. 2). We are in the process of testing the basis sets for solids as well and will report the corresponding results in a forthcoming paper. However, since solids are more dense systems than molecules or clusters and since our basis sets are explicitly constructed with a minimum BSSE, we expect them to work at least as well for solids as they do for molecules and clusters.

RMS errors of bond lengths and bond angles have been determined for the 14 selected test systems. Bond angles are described very accurately with all basis sets except for the 2.0 degree deviation of 6-31G* for water. It is more difficult to accurately describe this molecule with a small basis due to the existence of the lone electron pair on the oxygen atom. However, it is worth noting that DFO-R predicts 104.7° for the HOH angle which is very close to the experimentally determined angle of 104.5°. Bond lengths are very well converged (RMS errors of 0.002 Å or less) within both DFO basis sets for the molecules containing first-row elements. AG and 6-31G* show significantly larger errors of about 0.01 Å. Deviations in the bond lengths will very often lead to substantial errors in calculated vibrational frequencies. For example, the harmonic frequencies for the GGA-PBE symmetric stretching mode in H_2O are 3697 cm^{-1} and 3608 cm^{-1} if calculated using DFO-R and 6-31G*, respectively. Most of this error is due to different equilibrium geometries for the two basis sets.

The DFO-1 and DFO-2 absolute deviations for the systems containing Si and Mn atoms are larger (about 0.003 Å to 0.007 Å) but one needs to keep in mind that the bonds in these structures are weaker and 1.5–1.8 times longer than the bonds in the molecules that contain only first-row atoms. Hence, the relative error is only slightly increased. Overall, the performance of both DFO-1 and DFO-2 is very satisfactory.

C. Dipole moments

The dipole moment represents the first moment of the charge densities and hence is a good indicator for its convergence with respect to basis-set size. Four of the systems presented here have nonzero dipole moments. Their basis-set dependence is shown in Table II. DFO-1 performs very well except for H_2O, which has the lone electron-pair problem

TABLE III. Atomization energies (D) as calculated within LDA and GGA-PBE. Errors and values for C_{60} are given per atom. AG basis sets are from Refs. [14,23], and 6-31G* sets are from Ref. [13].

	LDA					GGA-PBE				
	DFO-R	DFO-2	DFO-1	AG	6-31G*	DFO-R	DFO-2	DFO-1	AG	6-31G*
H_2	4.90	4.90	4.89	4.99	4.82	4.53	4.54	4.53	4.63	4.43
CH_4	20.02	20.01	19.98	20.18	19.78	18.20	18.19	18.17	18.37	17.95
C_2H_6	34.38	34.36	34.31	34.58	34.10	31.05	31.03	30.99	31.28	30.76
C_2H_4	27.37	27.35	27.28	27.33	27.17	24.74	24.72	24.67	24.75	24.54
C_2H_2	19.88	19.85	19.79	19.56	19.69	17.93	17.91	17.86	17.68	17.74
C_{60}	8.50	8.49	8.47	8.40	8.57	7.47	7.45	7.43	7.40	7.53
H_2O	11.54	11.52	11.40	11.48	11.06	10.16	10.15	10.04	10.12	9.69
HCN	15.59	15.56	15.51	15.20	15.47	14.09	14.07	14.02	13.78	13.98
HCOOH	25.85	25.80	25.69	25.52	25.82	22.62	22.57	22.47	22.36	22.58
Δ/atm		0.01	0.03	0.07	0.07		0.01	0.03	0.05	0.07
Si_2H_6	25.08	25.01	24.90		24.93	22.51	22.45	22.36		22.38
Si_4	14.29	14.23	14.23		14.05	12.39	12.34	12.37		12.17
Mn_2O_2	16.89	16.83	16.65	16.32		14.09	14.07	13.91	13.60	
Mn_4O_4	39.14	39.02	38.69	38.45		33.06	33.01	32.74	32.50	

TABLE IV. Total-energy differences for selected reactions. Note that these are not reaction enthalpies since zero-point motion effects are not included. AG basis sets are from Refs. [14,23] and 6-31G* sets are from Ref. [13].

	Functional	DFO-R	DFO-2	DFO-1	AG	6-31G*
$C_2H_2+H_2\rightarrow C_2H_4$	LDA	2.59	2.60	2.60	2.78	2.66
	GGA-PBE	2.28	2.27	2.28	2.44	2.37
$C_2H_4+H_2\rightarrow C_2H_6$	LDA	2.11	2.11	2.14	2.26	2.11
	GGA-PBE	1.78	1.77	1.79	1.90	1.79
$C_2H_6+H_2\rightarrow 2CH_4$	LDA	0.76	0.76	0.76	0.79	0.64
	GGA-PBE	0.82	0.81	0.82	0.83	0.71
$HCOOH+3H_2\rightarrow H_2O+CH_4$	LDA	2.55	2.55	2.42	2.65	1.62
	GGA-PBE	2.31	2.30	2.19	2.36	1.46
$2\ Mn_2O_2\rightarrow Mn_4O_4$	LDA	5.36	5.36	5.39	5.81	
	GGA-PBE	4.88	4.87	4.92	5.30	

mentioned earlier. DFO-2 corrects most of the DFO-1 error and yields an almost converged result. For all other systems, DFO-1 and DFO-2 work very well in contrast to AG and 6-31G*, which show larger deviations for HCF_3 and HCN. Note also that the convergence is similar for both LDA and GGA-PBE functionals.

D. Atomization and reaction energies

One of the most important tasks of quantum physics and chemistry is the prediction of the relative stability of different structures. In order to calculate such properties accurately, one usually needs to take pressure, entropy, and possibly other effects into account. However, the largest contribution to the binding-energy difference of two systems normally comes from the difference in the atomization energies of the two systems. Table III displays the calculated atomization energies for the 14 test structures presented here, defined as the total-energy difference between the condensed system and free atoms (i.e., neglecting effects due to zero-point motion). Again, the DFO basis sets perform better than AG and 6-31G*. While the agreement between DFO-2 and DFO-R is very good in all cases, DFO-1 shows larger errors for H_2O and the systems containing Si and Mn. However, the deviations are acceptable for a basis set of this size and substantially smaller than for AG and 6-31G*. Further, it should be noted that both DFO-1 and DFO-2 always underestimate the correct value. This should be the case since they are both based on total-energy optimizations of the free atom and hence basis-set superposition errors should be small. To explicitly show that this is indeed the case, we have determined the BSSE for all atoms in fluoroform. While the total BSSE is rather small for both DFO sets (0.019 eV and 0.006 eV for DFO-1 and DFO-2, respectively), AG gives a significantly larger error of 0.060 eV. 6-31G* shows the worst performance with a BSSE of 0.6 eV. Since each system will have a different BSSE, errors of this magnitude can severely alter the computational results of reaction energies. Table IV illustrates this problem using a few hydrogenation and cluster-cluster reactions. For example, the 6-31G* energy difference for the hydrogenation of formic acid is almost 1 eV too small. On the other hand, the DFO basis sets show a good convergence.

E. Performance issues

One of the points made in the Introduction of this paper is that Gaussian basis sets, which share exponents between different angular momenta, will be more efficient than others. Table V summarizes relative timings for the calculation of the Coulomb potential in C_{60}. While such numbers may slightly depend on the specific implementation of the problem, it is apparent that the DFO basis sets show a better performance, especially when accuracy and speed are considered together.

IV. CONCLUSION

We have introduced a scheme for the full optimization of CGTOs for density-functional calculations on extended systems. The method is based on a total-energy minimization procedure for free atoms and makes efficient use of the total-energy gradient with respect to the Gaussian exponents. The number of exponents is not fixed but determined by requiring a predefined accuracy of the total energy, which leads to basis sets of minimum BSSE. The definition of additional breathing and polarization functions is based on a minimum-energy principle as well. DFO sets of higher accuracy may be created by successively adding additional basis functions, following the same energy-minimization procedure. Results for molecules and clusters suggest that the DFO basis sets presented here can accurately and efficiently describe a vari-

TABLE V. Total number of GTOs and basis functions per atom and relative timings for the calculation of the Coulomb potential in C_{60}. AG basis sets are from Refs. [14,23] and 6-31G* sets are from Ref. [13].

	DFO-2	DFO-1	AG	6-31G*
Number of GTOs	9	12	17	11
Number of basis functions	34	21	21	21
Relative timings	1.80	1.00	3.70	1.10

ety of systems with both LDA and GGA functionals. In order to simplify the application of our method, the software, which implements the optimization procedure, is made public on the World Wide Web.

ACKNOWLEDGMENTS

We thank J. Kortus for many helpful discussions. D.V.P. gratefully acknowledges support from the Alexander-von-Humboldt Foundation of Germany. This work was supported in part by the ONR Molecular Design Institute under Grant No. N0001498WX20709.

APPENDIX

The basis-set data are published electronically: see Ref. [26]. In this supplementary document, we give the Gaussian exponents and coefficients of the DFO-1 and DFO-2 basis sets for all elements discussed here. Additionally, we provide a DFO-1-type basis set for Si to be used with the Bachelet-Hamann-Schluter (BHS) pseudopotential [30,31].

[1] R. Car and M. Parrinello, Phys. Rev. Lett. **55**, 2471 (1985).
[2] D. Sanchez Portal, P. Ordejon, E. Artacho, and J. M. Soler, Int. J. Quantum Chem. **65**, 453 (1997).
[3] S. Goedecker and O. V. Ivanov, Solid State Commun. **105**, 665 (1998).
[4] K. N. Kudin and G. E. Scuseria, Chem. Phys. Lett. **289**, 611 (1998).
[5] E. Wimmer, H. Krakauer, M. Weinert, and A. J. Freeman, Phys. Rev. B **24**, 864 (1981).
[6] O. K. Andersen, Phys. Rev. B **12**, 3060 (1975).
[7] J. C. Slater, Phys. Rev. **36**, 57 (1930).
[8] S. F. Boys, Proc. R. Soc. London, Ser. A **200**, 542 (1950).
[9] S. Huzinaga, J. Chem. Phys. **42**, 1293 (1965).
[10] E. E. Lafon and C. C. Lin, Phys. Rev. **152**, 579 (1966).
[11] G. S. Paynter and F. W. Averill, Phys. Rev. B **26**, 1781 (1982).
[12] B. I. Dunlap, J. W. Connolly, and J. R. Sabin, J. Chem. Phys. **71**, 3396 (1979).
[13] M. J. Frisch, G. W. Trucks, H. B. Schlegel, P. M. W. Gill, B. G. Johnson, M. A. Robb, J. R. Cheeseman, T. Keith, G. A. Petersson, J. A. Montgomery, K. Raghavachari, M. A. Al-Laham, V. G. Zakrzewski, J. V. Ortiz, J. B. Foresman, J. Cioslowski, B. B. Stefanov, A. Nanayakkara, M. Challacombe, C. Y. Peng, P. Y. Ayala, W. Chen, M. W. Wong, J. L. Andres, E. S. Replogle, R. Gomperts, R. L. Martin, D. J. Fox, J. S. Binkley, D. J. Defrees, J. Baker, J. P. Stewart, M. Head-Gordon, C. Gonzalez, and J. A. Pople. GAUSSIAN94 (Gaussian Inc., Pittsburgh, PA, 1994).
[14] J. Andzelm, E. Radzio, and D. R. Salahub, J. Comput. Chem. **6**, 520 (1985).
[15] M. R. Pederson and K. A. Jackson, Phys. Rev. B **41**, 7453 (1990).
[16] K. A. Jackson and M. R. Pederson, Phys. Rev. B **42**, 3276 (1990).
[17] R. Jones and A. Sayyash, J. Phys. C **19**, L653 (1986); R. Jones, *ibid.* **21**, 5735 (1988); Mol. Simul. **4**, 113 (1989).
[18] D. Vogel, P. Kruger, and J. Pollmann, Phys. Rev. B **8**, 3865 (1998).
[19] P. Mlynarski and D. R. Salahub, Phys. Rev. B **43**, 1399 (1991).
[20] S. F. Boys and I. Shavitt, Proc. R. Soc. London, Ser. A **254**, 487 (1960).
[21] W. J. Hehre, R. Ditchfield, and J. A. Pople, J. Chem. Phys. **53**, 932 (1970), and references therein.
[22] H. Tatewaki and S. Huzinaga, J. Chem. Phys. **71**, 4339 (1979).
[23] N. Godbout, D. R. Salahub, J. Andzelm, and E. Wimmer, Can. J. Chem. **70**, 560 (1992).
[24] K. Faegri, Jr. and J. Almlöf, J. Comput. Chem. **7**, 396 (1986).
[25] A. Schäfer, C. Huber, and R. Ahlrichs, J. Chem. Phys. **97**, 2571 (1992).
[26] See AIP Document No. E-PAPS:PLRAAN-60-071910 for the optimized basis set exponents and coefficients. E-PAPS document files may be retrieved free of charge from our FTP server (http://www.aip.org/pubservs/epaps.html) or from ftp.aip.org in the directory /epaps/. For further information, email: paps@aip.org or fax: 516-576-2223.
[27] P. Hohenberg and W. Kohn, Phys. Rev. **136**, B864 (1964).
[28] W. Kohn and L. J. Sham, Phys. Rev. **140**, A1133 (1965).
[29] M. R. Pederson, J. Q. Broughton, and B. M. Klein, Phys. Rev. B **38**, 3825 (1988).
[30] D. R. Hamann, M. Schlüter, and C. Chiang, Phys. Rev. Lett. **43**, 1494 (1979).
[31] G. B. Bachelet, D. R. Hamann, and M. Schlüter, Phys. Rev. B **26**, 4199 (1982).
[32] J. R. Thomas, B. J. DeLeeuw, G. Vacek, T. D. Crawford, Y. Yamaguchi, and H. F. Schaefer, J. Chem. Phys. **99**, 403 (1993).
[33] D. V. Porezag and M. R. Pederson, Phys. Rev. B **54**, 7830 (1996).
[34] J. P. Perdew, J. A. Chevary, S. H. Vosko, K. A. Jackson, M. R. Pederson, D. J. Singh, and C. Fiolhais, Phys. Rev. B **46**, 6671 (1992).
[35] J. P. Perdew, K. Burke, and M. Ernzerhof, Phys. Rev. Lett. **77**, 3865 (1996).
[36] R. Ditchfield, W. J. Hehre, and J. A. Pople, J. Chem. Phys. **54**, 724 (1971).
[37] B. G. Johnson, P. M. W. Gill, and J. A. Pople, J. Chem. Phys. **98**, 5612 (1993).
[38] J. Andzelm and E. Wimmer, J. Chem. Phys. **96**, 1280 (1992).
[39] R. Fournier, S. B. Sinnot, and A. E. DePristo, J. Chem. Phys. **97**, 4149 (1992).
[40] C. M. Rohlfing and K. Raghavachari, J. Chem. Phys. **96**, 2114 (1992).
[41] K. Jackson, M. R. Pederson, D. Porezag, Z. Hajnal, and T. Frauenheim, Phys. Rev. B **55**, 2549 (1997).
[42] H. Stuart, in *Zahlenwerte und Funktionen aus Physik, Chemie, Astronomie, Geophysik und Technik*, edited by A. Eucken and K. H. Hellwege, Landolt-Börnstein, Vol. I, Pt. 3 (Springer-Verlag, Berlin, 1951).